Experimental study of two-phase flow inside flat plate pulsating heat pipe operating under μ-gravity

Maksym SLOBODENIUK[1,2*], Vincent AYEL[1], Remi BERTOSSI[2], Cyril ROMESTANT[1], Yves BERTIN[1]

[1]Pprime Institute CNRS – ENSMA – Université de Poitiers, UPR 3346
86961 Futuroscope-Chasseneuil (FR)
[2]IPSA, Direction de la Recherche et de l'Innovation de l'IPSA
92120 Ivry-sur-Seine (FR)
[*](Corresponding author: maksym.slobodeniuk@ensma.fr)

Abstract – Flat plate pulsating heat pipe was experimentally investigated during 69th ESA Parabolic Flight Campaign. Thermo-fluidic measurements were realized as well two-phase flow visualization. During microgravity periods, FPPHP operated mostly in dry-out mode with liquid accumulation in the condensation zone. Flow reactivations accompanied with temperature drops and two-phase flow transitions were observed during some parabolas. From the measurement of menisci positions during transitions, modified Weber, Froude and Bond numbers concerning the actual velocities and accelerations of liquid plugs were used for flow transition analysis. A novel flow pattern map for pulsating heat pipe with rectangular channels is then introduced.

Nomenclature

a	acceleration, $m.s^{-2}$
Bo	Bond number
D	diameter, m
Fr	Froude number
L	length, m
T	temperature, ◦C
v	velocity, $m.s^{-1}$
We	Weber number
Greek symbols	
ρ	density, $kg.m^{-3}$
σ	surface tension, $N.m^{-1}$
Index and exponent	
b	bubble
l	liquid

1. Introduction

In recent years, miniaturization of electronics components has induced high heat fluxes generation. This fact coupled with strong requirements as compactness, massless and small energy consumption for the aerospace applications lead to challenging issues in the thermal management sector. Among high efficiency passive thermal management devices for electronic equipment [1], one of the most promising cooling technology under the ray of research and development is the pulsating heat pipe (PHP). PHPs are thermally driven two-phase passive devices based on phase change induced liquid motion and capillary forces: liquid/vapour intermittent slug flow oscillates in a single capillary tube wound between hot and cold sources. Pressure instabilities in the evaporation zone initiate complex liquid flow, ranging from bubbly flow to slug/plug flow [2-4].

Thus, prediction of two-phase flows becomes a difficult challenge because available tools have been developed for systems in which mass flow rate is known, which is not the case in PHPs. Almost all available literature on flow visualization in PHPs is about qualitative analysis of flow behavior and of influence of sensible heat transfer on overall thermal performances, which are still contradictory [5,6].

https://doi.org/10.25855/SFT2022-109

Complex mechanisms of thermo-hydrodynamic processes inside PHPs are nor fully studied and any suitable design recommendations are not available, together with some contradictory assessments from researchers [7,8] and absence of universal flow transition criteria. Misunderstandings of relation between velocity and flow pattern need regular experimental investigations to be carried out.

Due to specific design features of flat plate pulsating heat pipes, as a plane shape which allows the installation of a transparent plate covering it, visualization studies are possible for all channels and zones without significant changes in fluid/structure interactions (besides, the base with milled channels is made from designed metallic material).

The general objective of this work is to study the flow behavior during stopover and following flow pattern transition during the reactivation phases.

2. Experimental System and Procedure

The flat plate pulsating heat pipe, developed for the thermal behavior and two-phase fluid flow characterization under microgravity conditions, consists of square shape serpentine channel (3×3 mm^2) with seven U-turns in evaporation zone, milled in molybdenum base plate ($80\times200\times3$ mm^3) and covered with sapphire transparent window allowing flow visualization (figure 1). Molybdenum was chosen as a construction material in order to have almost the same coefficient of thermal expansion (4.8 μm.K^{-1}) than sapphire glass (5.2 μm.K^{-1}), while maintaining a high thermal conductivity (138 W.m^{-1}K^{-1}).

Evaporator heating is ensured by the stainless still coated Ni-Chrome heating wire (Thermocoax® Type NcAc15) connected to ELC® ALR3220 power source (DC, 0-32 V, 0-10 A). Heat rejection from condenser was carried out thanks to a water circulation loop through the cooling plate embedded on the back side of the device (respecting condenser dimensions). Following water cooling was ensured with massive aluminum plate (air-cooled heat exchanger) equipped with fifteen microprocessor heat sinks. Ismatec® Reglo-ZS gear pump was used to force liquid circulation through condenser cooling block and aluminum heat exchanger.

T-type thermocouples (±0.7 K) were used for temperature measurements in evaporator, adiabatic section, inlet/outlet cooling water and ambient: four thermocouples were installed in the evaporator zone, between heating plate and FPPHP within the grooves milled inside channel ribs; and two thermocouples were glued on back side of the device in the center of the adiabatic zone. Measurements of the fluid pressure at the bottom of evaporator (connected to central U-turn) were realized with GE® PTX5076-TA digital pressure sensor (±200 Pa). Visualization of two-phase flow inside the device was realized via Canon® EOS 100D camera. Synchronization of recorded videos with other parameters was performed using LED, directly mounted on the PHP. Temperature and pressure data, as well gravity level, were acquired via NI® cRIO-9074 chassis with installed thermocouple and voltage inlet modules, and DC output module for synchronization procedure. The experimental system is schematically presented in fig. 1 (detailed description of the test section and experimental setup can be found in [9]).

Before filling procedure, leakage tests have been done using Pfeiffer Vacuum® Adixen ASM 142 helium leaks detector. Previous preliminarily terrestrial tests showed that molybdenum-water pair induces electrochemical reaction with generation of non-condensable gas and liquid/surface staining. Thus, pure ethanol was chosen as working fluid. Vacuumed PHP was filled with previously degassed ethanol with 40% of volumetric filling ratio (at 20°C).

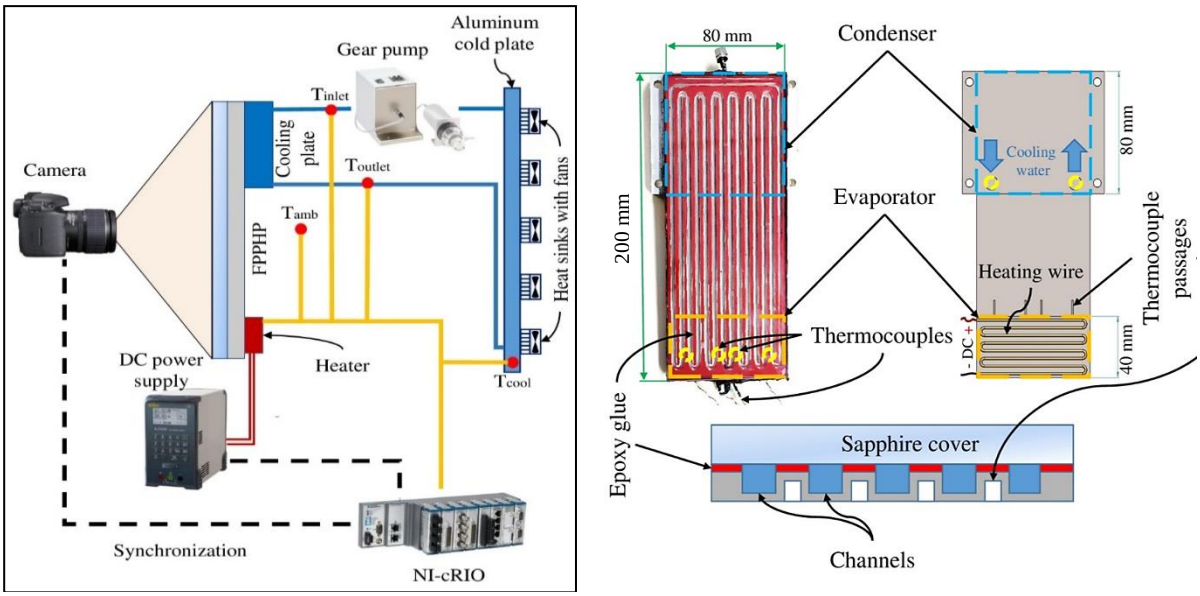

Figure 1: *Schematic view of the experimental system (left); and details of the FPPHP (right)*

Two computers are mounted into the main control rack for experimental system control, data acquisition and manipulations with camera. Developed LabView® software allows data acquisition and recording, trigger with camera for synchronization and input power regulation. Command systems also consist of security box (which is needed for partial or complete shutdown of experimental system in case of exceeding threshold temperature), self-made accelerometer and pump flow regulator. The main rack is connected to the onboard electrical system. The device was tested during ESA 69th parabolic flight campaign. During normal gravity periods, it operates in vertical position (BHM) due to normal gravity onboard of aircraft (the parabolic flight physics was described in details by Pletser et al [10]).

3. Results and Discussions

Fig. 2 depicts the temperature (red, orange and blue curves), pressure (gray curve) and gravity acceleration (dashed gray curve) profiles during one set of five consecutive parabolas for the FPPHP tested at 100 W of applied power. Just after each parabola starts, when microgravity conditions are reached, the evaporator temperatures drastically increase (ΔT) during the 22 s of microgravity, due to channel wall dry-out in the evaporator zone and liquid accumulation in the condenser zone (as showed in Fig. 3 – 0 s). This phenomena was observed for all tested heat loads applied (from 25 W to 150 W) during current work (graphics are not presented due to very similar temperature behavior, but average values of "ΔT" for all tested cases are shown in table 1). Adiabatic temperatures also smoothly increase during the beginning of the microgravity period – and heat is transferred mostly by conduction. Similarly to the adiabatic temperatures, pressure in evaporator slightly increases, probably due to evaporation of the residual liquid and vapor superheating. Sometimes, evaporator temperature drops during parabola were observed (fig. 2, parabola 3). At the same time, pressure and adiabatic temperature surges also can be observed, which illustrates the sudden change of the FPPHP operational mode – transition from stopover to oscillations, due to the two-phase fluid flow "re-activation" (as already observed in [9]).

Based on the observed temperature behavior of the FPPHP during microgravity periods, particularly during temperature drop and flow re-activation, two-phase flow comportment is of special interest to better understand the processes taking place inside the device. Fig. 3 presents three photographic prints of flow patterns inside the FPPHP during half second prior to re-

activation (Fig. 2, parabola 3): liquid accumulation in condenser in form of plugs is clearly seen in left picture (at t = 0 s); middle image shows the fluid distribution and liquid plugs displacement (red and blue rectangles) at t = 0.3 s; and right figure presents a "mixed" flow pattern just after re-activation (at t = 0.43 s), which includes four flow regimes in the form of bubbly, slug-plug, elongated slug (transition to annular) and semi-annular/annular flows.

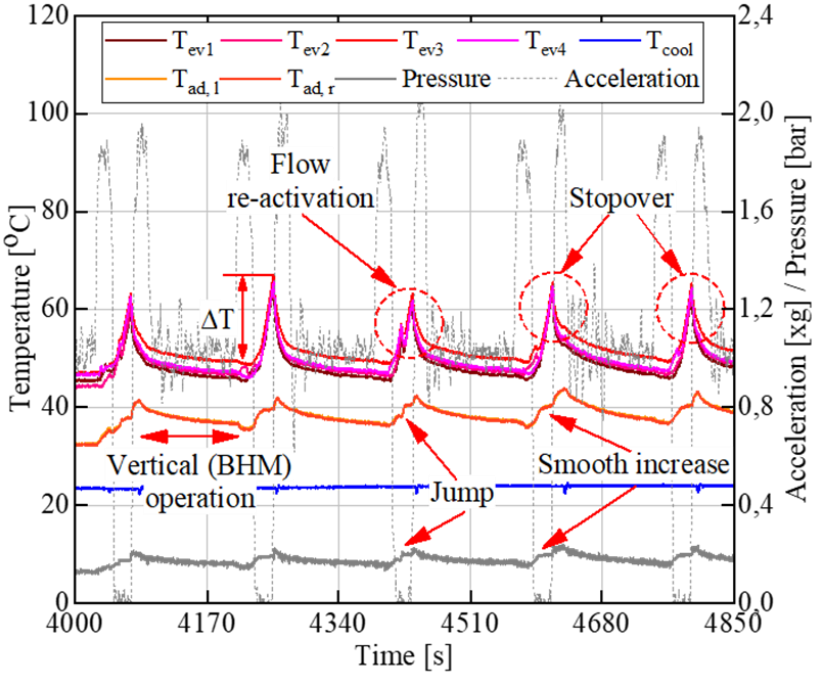

Figure 2: *Transient temperatures and pressure responses of the FPPHP related to the gravity acceleration changes at 100 W of heat load*

Heat load (W)	25	50	75	100	125	150
Average ΔT (K)	3	6	10	22	28	37

Table 1: *Average temperature drop values during parabola*

In previous work on flow transition during microgravity [9], a numerical tool was developed in order to understand the transition mechanism, allowing the vapor-liquid interface tracking prior to menisci deformation and/or their disappearance (flow regime transition). Knowing menisci positions for each image frame permits to determine their velocities and accelerations as functions of time until flow pattern change.

In general, extracted from videos menisci positions, velocity and acceleration profiles during microgravity periods look very similar to those presented in Fig. 4 (here for two successive channels, 8 and 9, connected by a U-turn in the condenser zone): from the start of the microgravity phase, the fluid flow operation could be divided in three periods: (1) transition from oscillations to stopover, (2) stopover establishment and (3) transition from stopover to oscillation mode. Beyond that, it is impossible to track the menisci, completely broken by very harsh fluid flow motion. First attempt to understand the recovery of oscillatory operation included hypothesis that liquid slugs penetrate in the evaporator zone and, due to their evaporation, lead to local pressure increases that force the startup of the overall motion. But, as can be seen from Fig. 4, liquid does not enter in the evaporator (bounded in the lower part by the dashed red line). Probably, activation of oscillatory motion of liquid plugs is provoked by liquid film evaporation in superheated adiabatic zone or non-uniform heating of evaporator.

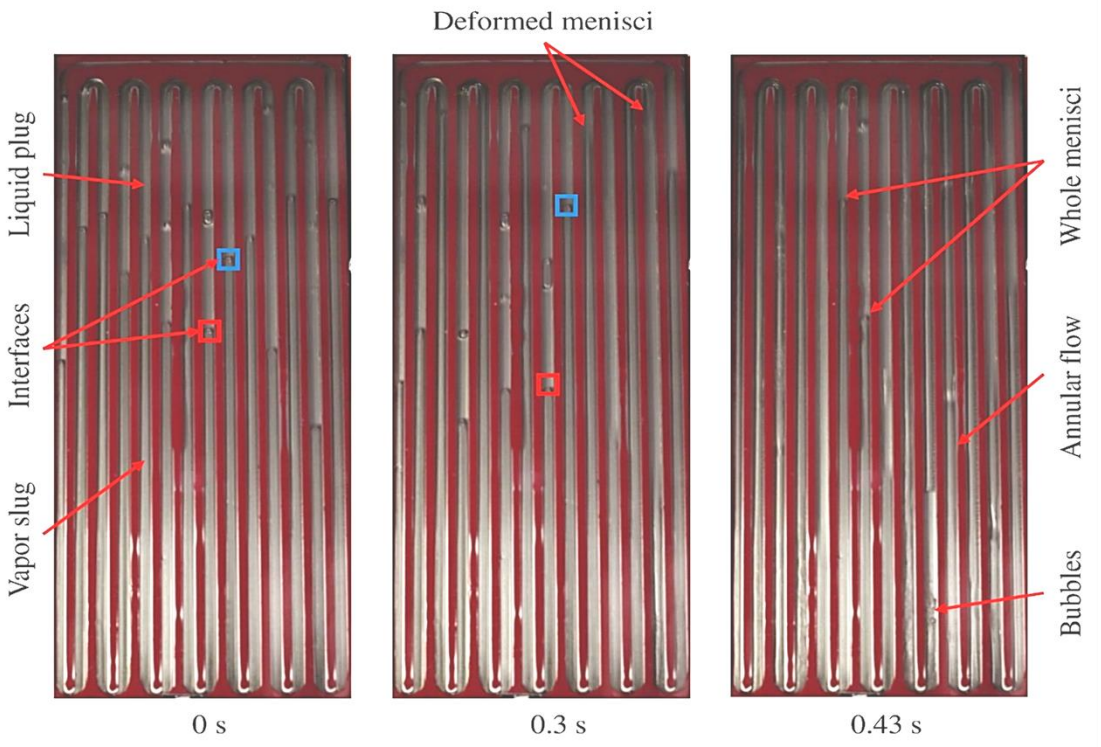

Figure 3: *Flow pattern inside the FPPHP during flow transition (100 W)*

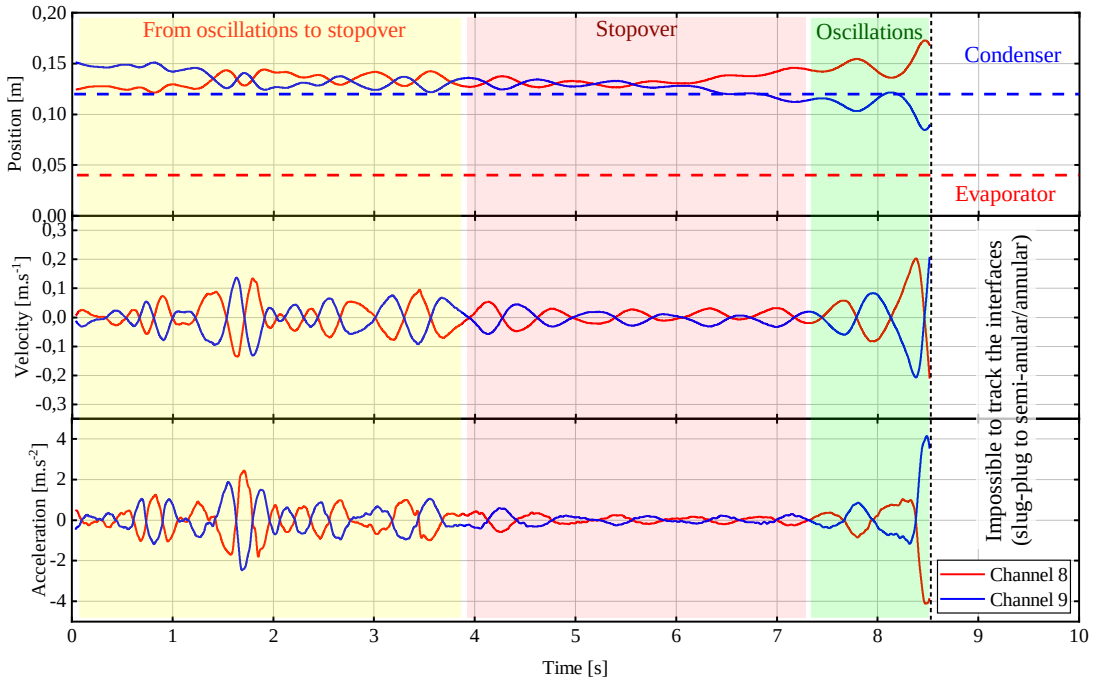

Figure 4: *Position, velocity and acceleration of liquid-vapor interfaces in two central neighboring channels (100 W)*

From velocities profiles of Fig. 4 it can be seen that, during period of transition to stopover, oscillation velocities almost do not exceed 0.1 $m.s^{-1}$, but they are very close to it. Menisci velocity amplitudes greatly decrease during stopover period and do not exceed the value of 0.03 $m.s^{-1}$. However, the main aim of this work is a quantitative characterization of the flow transition in FPPHP during microgravity and, looking back to the past researches, the most important is the transitional velocities and accelerations determination, from slug to semi-

annular-annular flow pattern, which can be defined here at the point before menisci deformation or disappearance (Fig. 5).

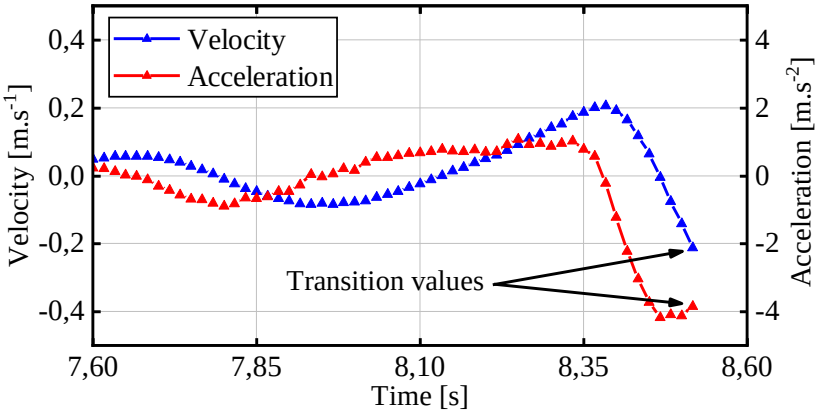

Figure 5: *Transient velocities and accelerations of liquid-vapor interface 1 s before flow transition from slug-pug to semi-annular/annular*

Defined transitional velocities, and accelerations, are in the range from 0.03 $m.s^{-1}$ to 0.5 $m.s^{-1}$, and from 0 $m.s^{-2}$ to 9.5 $m.s^{-2}$, respectively. Nevertheless, the corresponding average transitional velocities and accelerations are plotted in Fig. 6 as functions of heat load. The global increase in transitional velocities and accelerations with heat load can be explained by the evaporator superheat evolution leading to higher pressure differences during evaporation (main driving mechanism).

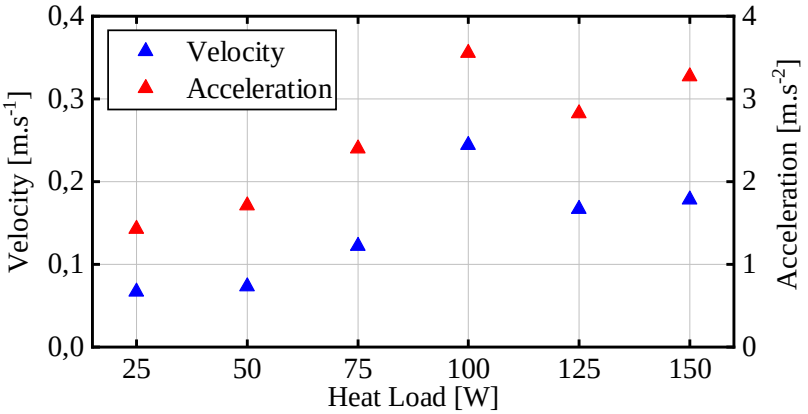

Figure 6: *Average velocities and accelerations distribution at transition from slug-plug to semi-annular/annular regime*

A universal definition of fluid flow pattern in pulsating heat pipes remains a big challenge due to the complex links between thermal and hydraulic operations. Existing correlations and flow pattern maps for slug-plug flows include known "input" parameters, like mass flow rate and vapor quality. Pietrasanta et al [11] proposed a first attempt of flow pattern map developed for thermally driven two-phase systems (i.e. a single-loop pulsating heat pipe) based on modified Weber (We), Bond (Bo) and Froude (Fr) numbers. The latter are used to express the ratios between inertial and surface tension forces, between external body forces and surface tension forces, and between momentum and external body forces, respectively. The modification from original numbers consists in replacing the gravity component g by actual acceleration (dv/dt) of menisci, and adding the ratio between bubble length L_b and channel diameter D. The modified We^*, Fr^* and Bo^* numbers were calculated as follow [11]:

$$We^* = \frac{\rho_l v^2 D}{\sigma}\left(\frac{L_b}{D}\right) \quad (1)$$

$$Fr^* = \frac{v}{\sqrt{\left(\frac{dv}{dt}\right)D\left(\frac{L_b}{D}\right)}} \tag{2}$$

$$Bo^{*0.5} = \left[\frac{\rho}{\sigma}\frac{dv}{dt}\right]^{0.5} D\left(\frac{L_b}{D}\right) \tag{3}$$

Regarding our experimental conditions in which liquid collects in condenser with almost equal lengths of liquid slugs, we used the same modified numbers, excluding component of bubble-length-to-channel-diameter ratio. Based on these modified non-dimensional numbers and experimentally obtained data-points, a novel flow pattern map is proposed for transition from slug-plug flow to semi-annular/annular using $Fr^{*0.25} \times We^{*0.25}$ as the ordinate and $Bo^{*0.5}$ as the abscissa (fig. 7). Also, data previously obtained for FPPHPs with 11 U-turns in evaporator, channel 3×3 mm^2 (200 W) and 1.5×1.5 mm^2 (50 W), and filled with FC72, is added to the plot.

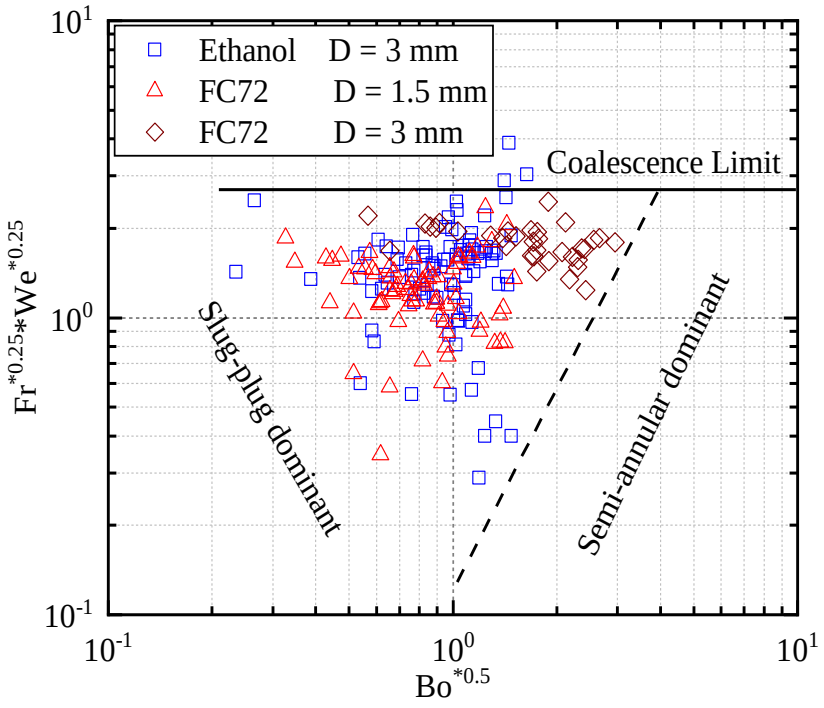

Figure 7: *Developed flow map for ethanol and FC72.*

Following the proposed flow patter map, the increase of $Fr^{*0.25} \times We^{*0.25}$ leads to the reduction in surface tension dominancy, resulting in bubble coalescence. The same can be concluded regarding transition from slug-plug to semi-annular/annular flow: with Bond number increase, the influence of surface tension decreases, provoking the flow transition.

Coalescence limit:

$$Fr^{*0.25} \times We^{*0.25} = 2.72 \tag{4}$$

Transition from slug-plug to annular:

$$Fr^{*0.25} \times We^{*0.25} = 0.125 \times (Bo^{*0.5})^{2.22} \tag{5}$$

Obtained correlations are quite different from proposed by Pietrasanta [11], probably due to higher complexity of given heat pipe, microgravity and rectangular channel shape which also influences on menisci formation. In addition, very narrow number of experimentally obtained data points provide a limited flow pattern map. Finally, the proposed correlations (Eq. (4-5)) and Fig. 7 can be used as a first step of limited flow regime map for predicting transitions in flat plate pulsating heat pipes operating in given conditions.

4. Conclusion

Thermal behavior and two-phase flow regimes in flat plate pulsating heat pipe operated under microgravity conditions were studied in this work. During microgravity periods, device mostly operated in dry-out mode. It was found that, during some parabolas, stop-over periods occur and are sometimes interrupted by a flow pattern transition from slug to annular flow, with uniform liquid distribution inside pulsating heat pipe, also called re-activation phases.

An object-tracking based visual analysis methodology has been developed, for liquid-vapor interfaces position determination, and was validated and implemented to study the flow behavior during stopover and re-activation periods under microgravity conditions.

A flow pattern map (based on modified Bond, Weber and Froude numbers including the actual fluid acceleration instead of constant gravity acceleration value), like that developed in [11], was adapted with results obtained during current work transitional velocities and accelerations of liquid plugs inside flat plate pulsating heat pipes with square channels.

References

[1] M. Mochizuki, Th. Nguyen, K. Mashiko, Y. Saito, T. Nguyen, V. Wuttijumnong, A review of heat pipe application including new opportunities, *Fr. Heat Pipes* 2 (2011) 1-15.

[2] S. Khandekar, P. Charoensawan, M. Groll, P. Terdtoon, Closed loop pulsating heat pipes, part B: visualization and semi-empirical modeling, *Appl. Th. Eng.* 23 (2003) 2021-2033.

[3] B. Tong, T. Wong, K. Ooi, Closed-loop pulsating heat pipe, *Appl. Th. Eng.* 21 (2001) 1845–1862.

[4] S. Liu, J. Li, X. Dong, H. Chen, Experimental study of flow patterns and improved configurations for pulsating heat pipes, *J. Therm. Sci.*16 (2007) 56–62.

[5] R. Senjaya, T. Inoue and Y. Suzuki, Oscillating Heat Pipe Simulation with Bubble Generation, *Proc. 15th Int. Heat Pipe Conf* (2010.).

[6] M. B. Shafii, A Faghri and Y. Zhang, Thermal Modeling of Unlooped and Looped Pulsating Heat Pipes., *ASME. J. Heat Trans.,* 123 (2001), 1159-1172.

[7] D. Bastakoti, H. Zhang, D. Li, W. Cai and F. Li, An overview on the developing trend of pulsating heat pipe and its performance., *Appl. Therm. Eng.* 141 (2018), 305-332.

[8] X. Tang, L. Sha, H. Zhang, Y. Ju, A review of recent experimental investigations and theoretical analyses for pulsating heat pipes., *Front. Energy.*, 7 (2013), 161-173.

[9] M. Slobodeniuk, R. Bertossi, V. Ayel, R. Ravichandran, K. Thyagarajan, C. Romestant and Yves Bertin, Experimental study of the flat plate pulsating heat pipe operation during dry-out and flow re-activation periods under microgravity conditions., *Int. J. Multiph. Flow*, 147 (2022), 103888.

[10] V. Pletser, S. Rouquette, U. Friedrich, J.-F. Clervoy, Th. Gharib, F. Gai and Ch. Mora, The First European Parabolic Flight Campaign with the Airbus A310 ZERO-G., *Microgravity Sci. Tech*., 28 (2016), 587–601.

[11] L. Pietrasanta, M. Mameli, D. Mangini, A. Georgoulas, N Michè, S. Filippeschi and M. Marengo, Developing flow pattern maps for accelerated two-phase capillary flows., *Exp. Therm. Fluid Sci*., 112 (2020), 109981.

Acknowledgements

This work was supported by European Space Agency in the framework of MAP INWIP and MAP TOPDESS research projects.